A Compact Eight-port CPW-fed UWB MIMO Antenna with Band-notched Characteristic

Li-Yan Chen, Wei-Si Zhou, Jing-Song Hong, and Muhammad Amin

Institute of Applied Physics, School of Physical
University of Electronic Science and Technology of China, 610054 Chengdu, China
727683316@qq.com, 1355746335@qq.com, cemlab@uestc.edu.cn, aminssphysics@hotmail.com

Abstract — A compact eight-port coplanar waveguide (CPW)-fed ultra-wideband (UWB) multiple-input-multiple-output (MIMO) antenna with band-notched characteristics in a small size of $54 \times 54 \times 0.8$ mm^3 is proposed in this paper. The eight-port MIMO antenna consists of four two-port MIMO antennas. For each two-port MIMO antenna, two monopole antenna elements are printed on the FR4 substrate and placed perpendicularly to each other. To increase impedance bandwidth and improve the isolation, a stub is positioned in the middle of two radiating elements. The band-notched characteristic are achieved by etching two L-shaped resonator slots on each radiating elements, respectively. The S_{11} reflection coefficients, coupling isolation, radiation patterns, peak gain and radiation efficiencies of the MIMO antenna are measured. The MIMO performance of the proposed antenna is analyzed and evaluated by the envelope correlation coefficient (ECC) and total active reflection coefficient (TARC).

Index Terms — Band-notched, CPW, ECC, MIMO, TARC, UWB.

I. INTRODUCTION

Since the Federal Communication Commission (FCC) assigned an unlicensed 3.1-10.6 GHz bandwidth, ultra-wideband (UWB) devices have been one of the most rapidly developing technologies in wireless applications due to its numerous blessings, including low power, high transmission rate, and so on [1-2]. The multipath fading in UWB system has been becoming more and more serious because of the low power limited by FCC. Multiple-input-multiple-output (MIMO) generation has incomparable advantages in improving the wireless link transmission capacity and reliability [3]. Therefore, combining MIMO technology with UWB technology is an efficient way to decrease multipath fading in UWB system [4]. However, there is a strong mutual coupling among two close radiating elements, which result in the loss of antenna bandwidth and radiating efficiency and make it difficult to design MIMO antenna in a compact dimension. Besides, the UWB overlaps with other wireless frequency bands, especially the wireless local area network (WLAN) frequency band at 5.15-5.85 GHz, which can cause some potential interference and noisy to the UWB system. Thus, it is inevitable to reduce both the mutual coupling among UWB MIMO antenna and the electromagnetic interference caused by WLAN system with some simple and effective methods.

Researchers have proposed various MIMO antennas [5-10]. Using electromagnetic band-gap (EBG) structure [5], or a tree-shaped parasitic structure [6], or a T-shaped protruded ground stub [7] to minimize the mutual coupling between radiating elements, or a complementary split-ring resonator (CSRR) etching on the antenna ground [8]. The MIMO antenna in [9] don't use any decoupling structure, the high isolation performance is achieved by the asymmetrical and complementary structures of the quasi-self-complementary antenna (QSCA). The antenna in [10] has the smallest dimension in those UWB MIMO antennas, etching a T-shaped slot at the antenna ground to enhance the impedance bandwidth and reduce the mutual coupling. However, the antenna in [5] is not suitable for UWB system due to their narrow operation band. The operation band of antennas in [6], [8], [9] and [10] is UWB level, but it can't avoid the noise and interference in WLAN band.

In this paper, a compact eight-port CPW-fed UWB MIMO slot antenna with WLAN band-notched characteristics in a size of $54 \times 54 \times 0.8$ mm^3 is presented. The eight-port MIMO antenna consists of four two-port MIMO antennas. Each two-port MIMO antenna consists of two orthorhombic monopole antenna fed by CPW. A ground stub which is protruded at 45° in the middle of two radiating elements acts as a reflector to achieve UWB characteristics and high isolation. To be able to acquire the band-rejected characteristics at WLAN operation band, a L-shaped slot resonators (approximately half wavelength at 5.5 GHz) are etched on each radiating element. The proposed UWB MIMO slot antenna is manufactured and measured, measured outcome show that the designed antenna exhibits $S_{11} < $ -10 dB, high isolation better than 17 dB, peak gain varies 1.524 dBi to

2.83 dBi, radiation efficiencies varies 74.7% to 85%, ECC < 0.02 and TARC < -15 dB over the whole UWB band except for a notched at 5-6 GHz. Compared to the previous UWB MIMO antennas in [5]-[10], this UWB MIMO slot antenna has the superiority of more ports, a notched band and better MIMO performance.

II. ANTENNA DESGIN

A. Antenna geometry

The geometry and photograph of the proposed eight-port MIMO antenna which consists of four two-port MIMO antennas is illustrated in Fig. 1. The antenna is engraved on a 54×54×0.8 mm^3 square FR4 (dielectric constant of 4.4 and loss tangent of 0.02) substrate. All parameters are in millimeter and optimized by simulating in ANSYS Electromagnetics Suite 17.1, as shown in Fig. 1.
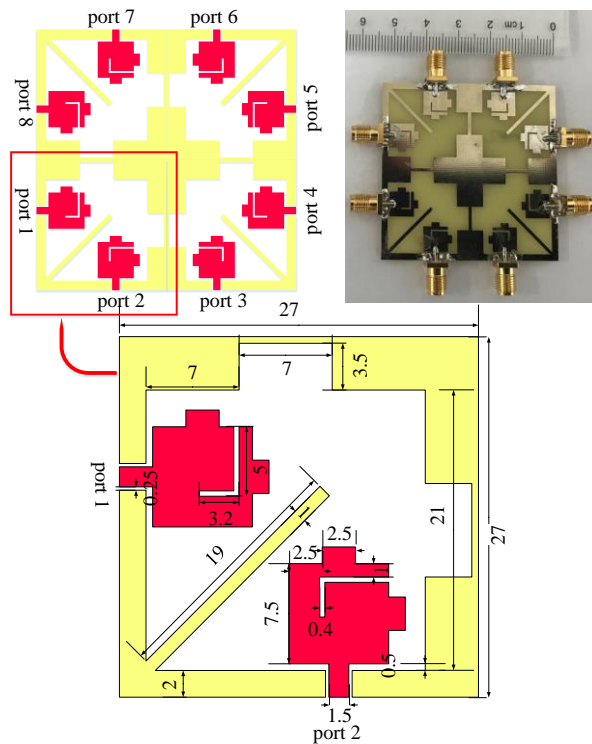
Fig. 1. The geometry and photograph of the proposed UWB MIMO antenna.

B. The two-port MIMO slot antenna

The design process of the presented MIMO slot antenna is demonstrated in Fig. 2, including antennas I-IV. The simulated S-parameters of antenna I-IV are shown in Fig. 3. First, antenna I which consists of two orthorhombic square monopole antennas is presented. A square slot is etched on the ground to obtain a wide operation band. The fundamental resonant frequency f_r

of antenna I can be estimated by (1) [11]:

$$f_r = \frac{144}{l_1 + l_2 + g + \frac{A_1}{2\pi l_1 \sqrt{\varepsilon_{re}}} + \frac{A_2}{2\pi l_2 \sqrt{\varepsilon_{re}}}}, \quad (1)$$

where l_1 and A_1 denote the length and area of the radiation patch, respectively, l_2 and A_2 denote the length and area of the ground, g is the gap between the ground and the radiation patch. For antenna I, $l_1 = Lb$, $l_2 = La$, $g = g$, $A_1 = Lb \times Lb$ and $A_2 = Lg \times (L/2 - Wf - 2t) + (L - Lg - La) \times La$. ε_{re} is the effective dielectric constant of FR4 and $\varepsilon_{re} = \frac{\varepsilon_r + 1}{2}$. The calculated fr is 4.8 GHz, the simulated fr is about 5 GHz, which is very close to the calculated value using formula (1).

Then, on the basis of antenna I, protruding two parasitic rectangular stubs on square radiation patches and etching two additional rectangular slots on the ground, as illustrated as antenna II. The antenna II exhibits a wider operational bandwidth than antenna I, especially in the low spectrum, but it still can't reach the UWB level. Finally, a ground stub is extended at 45° in the middle of two radiating elements of antenna II to further expand bandwidth, as shown in antenna III. The ground stub acts as a reflector to make the first resonator move from 5.4 GHz to 3.8 GHz, as the blue $S_{11/22}$ curve shown in Fig. 3. Therefore, the UWB characteristics have achieved.
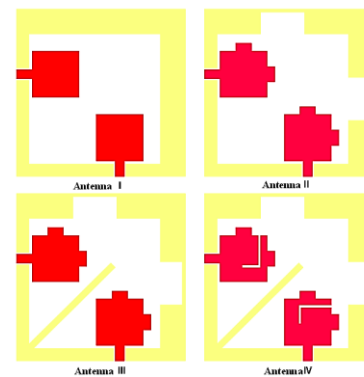
Fig. 2. The design process of proposed UWB MIMO slot antenna.

(a)

(b)
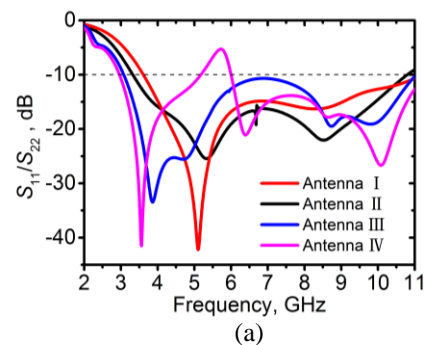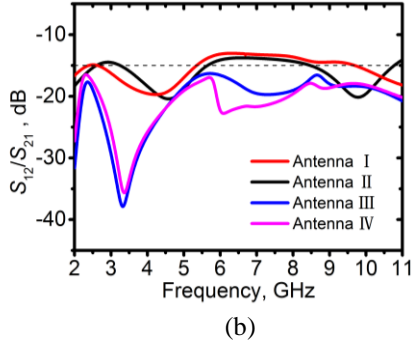
Fig. 3. Simulated S11/S22 parameters of Antenna I-IV (a), and Simulated S12/S21 parameters of Antenna I-IV (b).

C. Achievement of decoupling

Although the two radiation elements in antenna I and II are placed perpendicularly to one another, the coupling between two excited ports remains worse in middle spectrum. The ground stub in antenna III acts as a reflector which separates the two radiating elements to decrease the mutual coupling between the two ports. The $S_{12/21}$ isolation results are improved to more than 17 dB by the addition of stub, as can be seen from the blue $S_{12/21}$ curve illustrated in Fig. 3.

In order to further understand the function of the ground stub, Fig. 4 shows the surface current distributions at 7 GHz without and with the stub when port 1 is excited. Most of the current is accumulating on the excited port and the stub. The stub prevents current flowing from port 1 to port 2, resulting in high isolation.

(a)   (b)
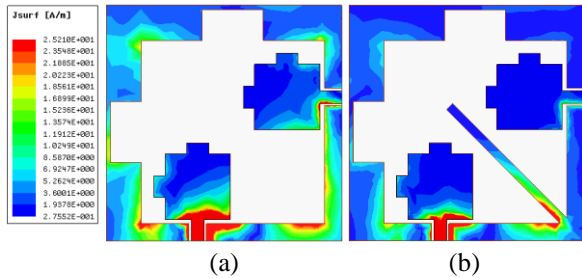
Fig. 4. Surface current distributions of antenna II (a), and antenna III at 7 GHz (b).

D. Achievement of band-notched characteristics

The band-notched characteristics of WLAN spectrum (5.15 GHz-5.85 GHz) for the presented UWB MIMO antenna is accomplished by etching an L-shaped slot on each radiating element of the antenna III, as shown in antenna IV of Fig. 2. The length of the slot is about quarter wavelength corresponding to 5.5 GHz and estimated by the formula (2) [12]:

$$l1 + w1 = \frac{c}{4f_0\sqrt{\varepsilon_{re}}}, \qquad (2)$$

where c is the velocity of the light, $\varepsilon_{re} = \frac{\varepsilon_r+1}{2}$ is the relative dielectric constant of FR4. The calculated $l1 + w1$ is 8.4 mm approximately.

Figure 5 (a) illustrates the simulated S-parameters for different values of $l1 + w1$. The rejected band is shifting to the low frequency with the increase of value of $l1 + w1$, but almost no impact on $S_{12/21}$ isolation. The value of $l1 + w1$ is selected to 8.2 mm for obtaining notched band from 5 GHz to 6 GHz.

Figure 5 (b) shows the surface current distributions at 5.5 GHz of antenna IV when port 1 is excited. A large amount of current has trapped in the L-shaped slot, which acts as a capacitance to obtain the band-notched characteristics.

(a)

(b)
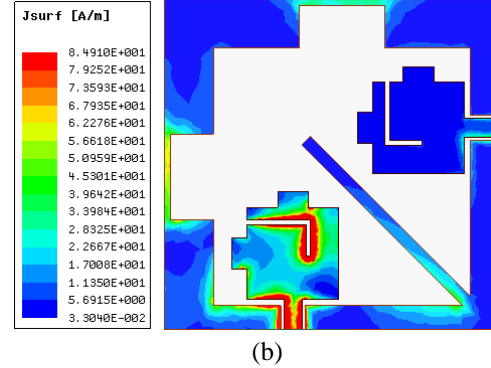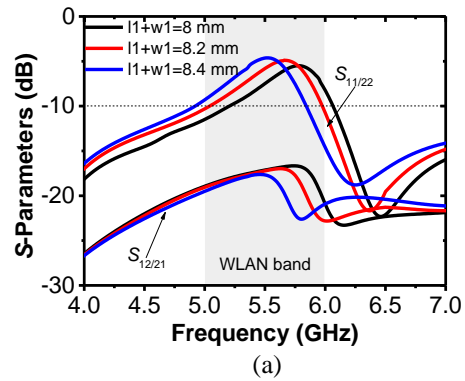
Fig. 5. Simulated S-parameters for different $l1 + w1$ (a), and surface current distributions of antenna IV at 5.5 GHz (b).

III. MEASURED RESULTS

The proposed eight-port UWB MIMO slot antenna has fabricated and measured to verify the simulation results. The port 1 is measured and other ports ceased with a 50 Ω load during the measurement.

A. S-parameters

The S-parameters of the fabricated antenna are presented in Figs. 6-7. There is a superb settlement between simulated and measured results. Some discrepancies

can be seen, which may be caused by the manufacture tolerance, SMA connector and the fluctuation of the dielectric constant of FR4. Measured outcomes show that the proposed MIMO antenna operates from about 3.1 GHz to 11 GHz with $S_{11/22} < -10$ dB except for a notched band from 5 GHz to 6 GHz and $S_{12\text{-}18} < \text{-}15$ dB.
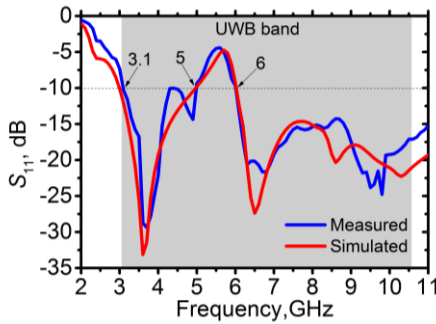
Fig. 6. The measured and simulated S_{11} of the eight-port UWB MIMO antenna.
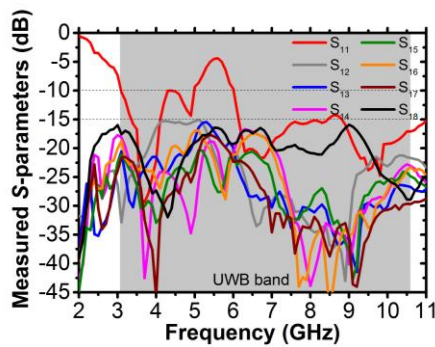
Fig. 7. The measured S-parameters of the eight-port UWB MIMO antenna.

B. Radiation performance

Three frequency points (4 GHz, 7 GHz, and 10 GHz) are selected to indicate the radiation pattern for low frequency, middle frequency and high frequency in the UWB band, respectively. Figures 8 (a-c) illustrate the radiation pattern of UWB MIMO antenna in E-plane (xoz-plane) and H-plane (xoy-plane). It can be realized that the radiation pattern in both E-plane and H-plane are quasi-omnidirectional. Besides this, the peak gain and radiation efficiencies of the proposed MIMO antenna is shown in Fig. 8 (d). The peak gain varies 1.524 dBi to 2.83 dBi and radiation efficiencies varies 74.7% to 85% over the UWB spectrum except for the notched band. At the notched band (5.15 GHz-5.85 GHz), there is a deep drop in Peak Gain, this dramatical drop in gain enables the antenna to avoid crosstalk from signals in WLAN band and operate in the high interference surroundings.
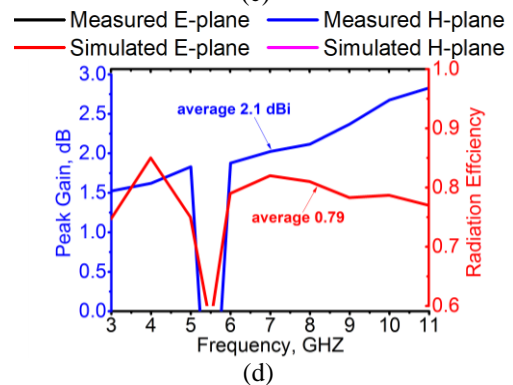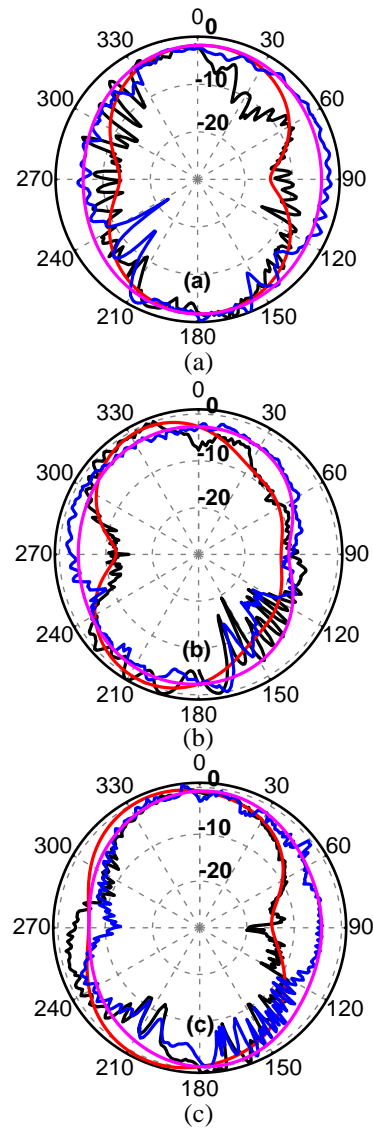
Fig. 8. Simulated and measured radiation pattern of the UWB MIMO slot antenna at: (a) 4 GHz, (b) 7 GHz, (c) and 10 GHz. (d) The measured peak gain and radiation efficiencies of the UWB MIMO slot antenna vs frequency.

C. MIMO performance

The MIMO performance of the proposed antenna is analyzed and figured out by the ECC and TARC. The value of ECC signifies how the two antennas are coupled to each other. For achieving good channel characteristics and antenna diversity, the ECC must be less than 0.05. The ECC between two elements can be calculated from the S-parameters using the formula (3) when the radiation efficiency of the MIMO antenna is high [13]:

$$ECC = \frac{|S_{11}^* S_{12} + S_{21}^* S_{22}|^2}{(1 - |S_{11}|^2 - |S_{12}|^2)(1 - |S_{21}|^2 - |S_{22}|^2)}. \quad (3)$$

For MIMO antenna systems, traditional scattering matrixes are not sufficient to predict the real antenna performance. TARC which take coupling effect into account has been proposed. The TARC for the 8-port MIMO antenna could be described as [14]:

$$TARC = -\sqrt{\left(\sum_{i=1}^{8} \left(\sum_{k=1}^{8} S_{ik}\right)^2\right)/8}. \quad (4)$$

As depicted in Fig. 9, the measured ECC is less than 0.02 and TARC is less than -20 dB for the UWB band.
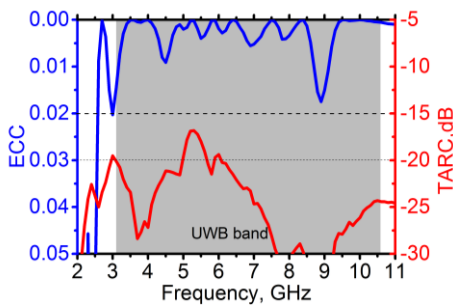
Fig. 9. Measured ECC and TARC of the proposed UWB MIMO antenna against frequency.

IV. CONCLUSION

In this paper, a compact eight-port UWB MIMO antenna with WLAN band-notched characteristics in a size of $54 \times 54 \times 0.8$ mm^3 has been designed successfully. Measured outcomes show that the designed antenna exhibits $S_{11} < -10$ dB, high isolation better than 15 dB, peak gain varies 1.524 dBi to 2.83 dBi, radiation efficiencies varies 74.7% to 85%, ECC < 0.02 and TARC < -20 dB over the UWB band except for a notched band at 5-6 GHz. In addition, the proposed scheme retains full planarity of the UWB MIMO antenna, involves simple and straightforward fabrication process. All the measured, simulated and calculated results indicate the proposed eight-port MIMO antenna is a good candidate for UWB system.

REFERENCES

[1] Federal Communication Commission, "First report and order Revision of part 15 of the Commission's rules regarding ultra-wideband transmission system," *FCC 02 48*, 2002.

[2] I. Oppermann, M. Hamalainen, and J. Iinatti, *UWB Theory and Applications.* New York: Wiley, ch. 1, pp. 3-4, 2004.

[3] A. J. Paulraj, D. A. Gore, R. U. Nabar, and H. Bolcskei, "An overview of MIMO communications-A key to gigabit wireless," *Proceedings of the IEEE*, vol. 92, pp. 198-218, 2004.

[4] T. Kaiser, F. Zheng, and E. Dimitrov, "An overview of ultrawide-band systems with MIMO," *Proceedings of the IEEE*, vol. 97, pp. 285-312, 2009.

[5] Q. Li, A. P. Feresidis, M. Mavridou, and P. S. Hall, "Miniaturized double-layer EBG structures for broadband mutual coupling reduction between UWB monopoles," *IEEE Transactions on Antennas & Propagation*, vol. 63, no. 2, pp. 1168-1171, 2015.

[6] S. Zhang, Z. Ying, J. Xiong, and S. He, "Ultra-wideband MIMO/diversity antennas with a tree-like structure to enhance wideband isolation," *IEEE Antennas Wireless and Propagation Letters*, vol. 8, pp. 1279-1282, 2009.

[7] L. Liu, S. W. Cheung, and T. I. Yuk, "Compact MIMO antenna for portable UWB applications with band-notched characteristic," [J]. *IEEE Transactions on Antennas & Propagation*, vol. 63, no. 3, pp. 1917-1924, 2015.

[8] M. S. Khan, A. Capobianco, S. M. Asif, D. E. Anagnostou, R. M. Shubair, and B. D. Braaten, "A compact CSRR enabled UWB diversity antenna," *IEEE Antennas & Wireless Propagation Letters*, 2016.

[9] X. L. Liu, Z. D. Wang, Y. Z. Yin, J. Ren, and J. J. Wu, "A compact ultra-wideband MIMO antenna using QSCA for high isolation," [J]. *IEEE Antennas & Wireless Propagation Letters*, vol. 13, pp. 1497-1500, 2014.

[10] C. M. Luo, J. S. Hong, and L. L. Zhong, "Isolation enhancement of a very compact UWB-MIMO slot antenna with two defected ground structures," [J]. *IEEE Antennas & Wireless Propagation Letters*, vol. 14, pp. 1766-1769, 2015.

[11] K. G. Thomas and M. Sreenivasan, "A simple ultrawideband planar rectangular printed antenna with band dispensation," *IEEE Trans. Antennas Propag.*, vol. 58, no. 1, pp. 27-34, Jan. 2010.

[12] R. Chandel, A. K. Gautam, and K. Rambabu, "Tapered fed compact UWB MIMO-diversity antenna with dual band-notched characteristics," *IEEE Transactions on Antennas & Propagation*, vol. 1, no. 1, pp. 99-107, 2018.

[13] S. Blanch, J. Romeu, and I. Corbella, "Exact representation of antenna system diversity performance from input parameter description," *Electron. Lett.*, vol. 39, no. 9, pp. 705-707, 2003.

[14] S. I. Jafri, R. Saleem, M. F. Shafique, and A. K. Brown, "Compact reconfigurable multiple-input

multiple-output antenna for ultra wideband applications," *IET Microwaves, Antennas & Propagation*, vol. 10, pp. 413-419, 2015.

Jing-song Hong received the B.Sc. degree in Electromagnetics from Lanzhou University, China, in 1991, and the M.Sc. and Ph. D. degrees in Electrical Engineering from the University of Electronic Science and Technology of China (UESTC), in 2000 and 2005, respectively. From 1999 to 2002, he was a Research Assistant with the City University of Hong Kong. He is now a Professor with UESTC. His research interest includes the use of numerical techniques in electromagnetics and the use of microwave methods for materials characterization and processing.

Li-yan Chen was born in Wuhan, China. He received his B.S. degree from Shanxi University in 2016. He is now working towards his M.S. degree in Radio Physics at the University of Electronic Science and Technology of China (UESTC). His interests include MIMO antenna and MIMO system.

Wei-si Zhou was born in Anqing, China. He received his Bachelor degree from Shandong University of Technology in 2018. Since September 2018 he is a master student in the major of Electronics and Communications Engineering at the University of Electronic Science and Technology of China (UESTC). His interests include MIMO antenna and UWB antenna.

Muhammad Amin was born in D.I.Khan, Pakistan. He received his master degree from Gomal University D.I.Khan Pakistan in 2003. Since September 2014 he is a Ph.D. student in the major of Radio Physics at the University of Electronic Science and Technology of China (UESTC). His interests include antenna technology and wireless communication technology.